Continuous Carbon Nanotube-based Fibers & Films for Applications Requiring Enhanced Heat Dissipation

Peng Liu, [†, ‡] Zeng Fan, [‡] Anastasiia Mikhalchan, [‡] Thang Q. Tran, [‡] Daniel Jewell, [§] Hai M. Duong, [‡,*] and Amy M. Marconnet [†,*]

[†]School of Mechanical Engineering and the Birck Nanotechnology Center, Purdue University, West Lafayette, Indiana, United States

[‡]Department of Mechanical Engineering, National University of Singapore, 9 Engineering Drive 1, EA-07-05,Singapore 117575, Singapore

[§]Department of Materials Science and Metallurgy, University of Cambridge, United Kingdom

*Corresponding authors: Amy M. Marconnet: amarconn@purdue.edu, Hai M. Duong: mpedhm@nus.edu.sg.

1. Validation of one-dimensional heat transfer along the length of the fiber:

As shown in Figure S1a, we select a region whose width is slightly smaller than that of the fiber to avoid the influence of the temperature of the air near the edge of the fiber, as shown as the faint white box in Figure S1a. In this example, a 35×876 matrix of data is generated as the temperature profile along the wire. Here, we plot all the 35 rows of pixels at different y positions (across the cross section) within the box in panel a. The average of these 35 rows is also plotted in Figure S1b as the green dots. As we can see, the temperature variation is ~±0.5 °C and the all curves fall within the same range. For a clearer comparison, we choose 3 typical positions (Row 10 is around ¼ width from the edge, Row 34 is near the edge and Row 19 is near the center of the wire). As shown in Figure S1c, the temperatures measured at these three rows are not significantly different, which confirms the validity of the 1-D assumption.
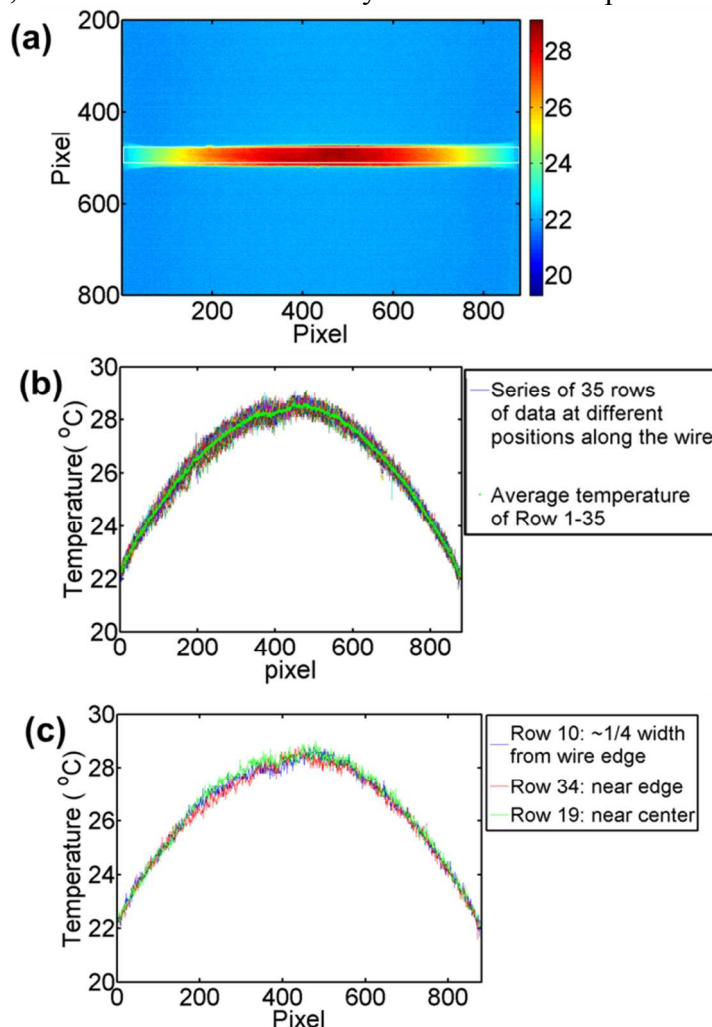
Figure S1. (a) Example infrared microscope image of a CNT fiber during Joule heating. The faint white box indicates the region selected for analysis. (b) Temperature profile for 35 rows of pixels within the box in panel a. Note that the noise in the temperature data is ~±0.5 °C and the all curves fall within the same range. (c) Temperature curves of 3 selected rows of pixels from panel a. (Row 10 is ~ ¼ width from the edge, Row 34 is at the edge, and Row 19 approximately the center of the wire).

2. Emissivity Calibration & Thermal Image Acquisition:

A two-step process is required to calibrate the infrared microscope and obtain accurate thermal data from the measured radiance data.

We first measure the emissivity of the fibers at a constant, uniform temperature. Specifically, as recommended Quantum Focus Instruments (the manufacturer of the IR microscope), the emissivity of the sample is measured at an elevated temperature (80 °C) by heating the fiber using a hot plate. The fiber temperature is confirmed using a T-type thermocouple. When the temperature is stable, the radiance incident on each pixel of the detector is measured and compared to that of a blackbody at 80 °C in order to estimate the emissivity (of radiation in the range of 2 -5 μm). To confirm the accuracy of this measured emissivity, the sample is then cooled to uniform temperatures of 60 °C, 40°C and room temperate (22 °C). At each temperature, a thermal image of the sample is acquired assuming the measured emissivity at 80°C. The temperature extracted from the mapping image is compared to that measured by the T-type thermocouple. If the difference between the two temperatures are within 1°C, we regard the emissivity is valid. In this work, the emissivity of the samples is measured as 0.86±0.02.

Once the sample emissivity is measured, thermal data is acquired for the suspended samples. Specifically, the sample is first suspended at room temperature without current flow and a reference radiance map is acquired. Then, the sample is heated by Joule heating. The change in measured radiance, combined with the measured emissivity, enable extraction of the temperature of each pixel in the image. The reference image at uniform, room temperature is required to account for the reflected radiation from surroundings.

3. The influence of variable local heat transfer coefficient on the temperature profile of the wire:

The local heat transfer coefficient may vary along the wire, but the influence of variable local heat transfer coefficient ($h(T)$) on the temperature profile of the wire ($T(x)$) is very slight. The range of currents tested is limited to ensure the average temperatures of the specimens do not exceed 303.5 K (just a few degrees above room temperature of 295.15). Typically, the average temperature is 299.15 K. Here, the temperature profile used as an example is extracted from a solid NiCr wire (D=254 μm, k=13 W m^{-1} K^{-1}, AWG 30, Consolidated Electronic Wire & Cable, United States).

First, we assume the convective coefficient is a constant ($h_{constant}$) along the entire wire and fit the experimental temperature (see the green dots in Figure S2a) with the Equation 6 and 7 in the manuscript (see the red solid line in Figure S2a). We obtain a thermal conductivity of 12.8 W m^{-1} K^{-1} and a natural convective coefficient of 59.6 W m^{-2} K^{-1}. Note that the convective coefficient of 59.6 W m^{-2} K^{-1} is comparable with 57.5 W m^{-2} K^{-1} calculated from Churchill-Chu correlation using the average temperature of the wire (29 °C).

Second, we calculate and plot the temperature-dependent convective coefficient ($h(T)$) in Figure S2b using Churchill-Chu correlation[1] and Thermophysical Properties of Gases at Atmospheric Pressure[1]. Then we plot the temperautre curve (see the blue dash line in Figure S2a) using Equation 6 in the manuscript with the temperature-dependent convective coefficient ($h(T)$) at each x position. Note that the deviations of the temperature curves calculated using $h_{constant}$

and $h(T)$ respectively are very small. In addition, the average of $h(T)$ is 57.2 W m^{-2} K^{-1} which is also close to $h_{constant}$ (59.6 W m^{-2} K^{-1}).

Hence, we assume a constant convective coefficient along the wire when the temperature rise in the wire itself is limited to a few Kelvin above the set base temperature.

For the CNT fiber sample, the average temperature of the fiber in Figure S1 is 299.15 K. We can see that the highest temperature along the fiber is no more than 302.5 K. Based on the estimates of the Churchill-Chu correlation, this range of temperature variation does not have a significant impact on the magnitude of the heat transfer coefficient. The small variations in $h(T)$ along the length of the fiber enable an approximation that the heat transfer coefficient is constant: $h(T(x)) \approx h(299.15K)$.
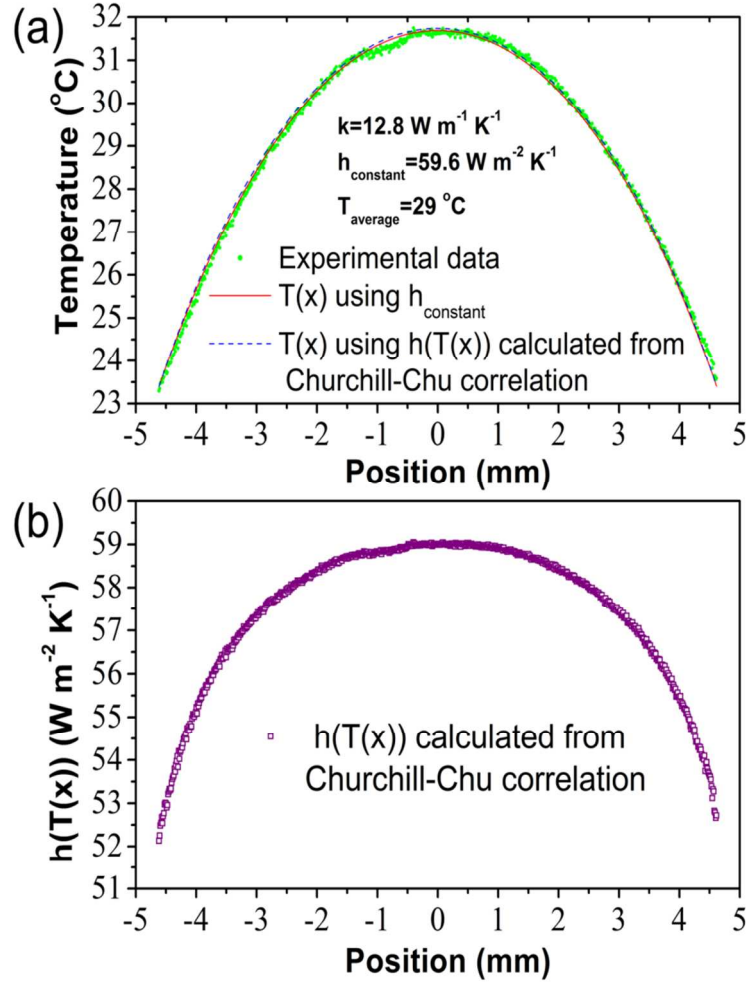
Figure S2. (a) Temperature profile along a NiCr wire. Green dots show the experimental data for the NiCr wire with an average temperature of 29°C; the red solid line shows the temperature profile calculated from Equation 1 assuming the convective coefficient is a constant ($h_{constant}$ = 59.6 W m^{-2} K^{-1}) and a thermal conductivity of 12.8 W m^{-1} K^{-1}; and the blue dashed line shows the calculated temperature profile assuming the convective coefficient is a function of temperature ($h(T)$). Note that the deviations of temperature profiles calculated using $h_{constant}$ and $h(T)$ are very small. (b) Convective heat transfer

coefficient as a function of position along the wire as calculated from Churchill-Chu correlation.

4. The variation of the convective coefficients from Churchill-Chu correlation with average fiber temperatures in the range of 296.15 K-303.15 K:
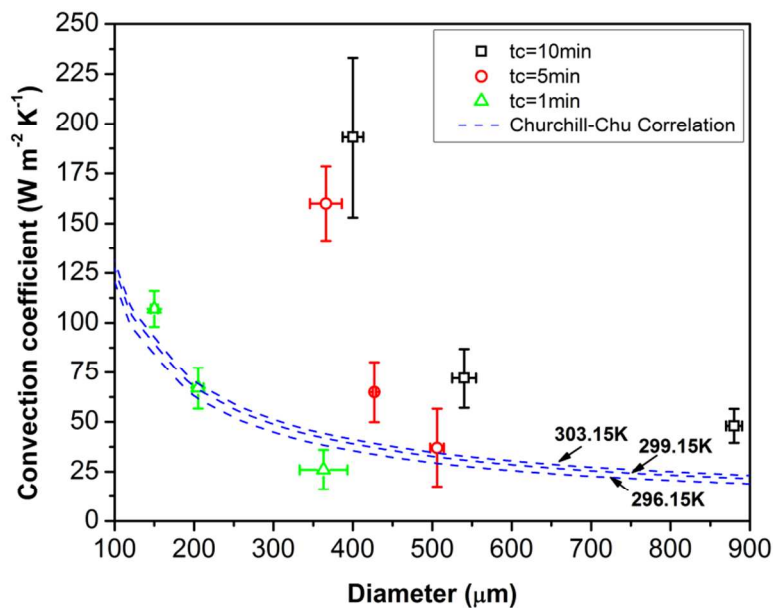
Figure S3. Comparison of the convective coefficient between the experimental results and those calculated from Churchill-Chu correlation. Note that the deviations from Churchill's correlation within 296.15 K-303.15 K are not significant.

5. Summary of the properties of the CNT fibers:

Table S1. Properties of CNT fibers discussed in the primary article.

Collecting time (min)	Diameter (μm)	Density (g cm^{-3})	Volume fraction (%)	Electrical conductivity (S cm^{-1})	Thermal conductivity (W m^{-1}K^{-1})	Convective coefficient (W m^{-2} K^{-1})
			As-prepared fiber			
10	880±10	0.15±0.01	7.1±0.3	230±20	5.1±0.4	48±9
10	540±15	0.37±0.01	17.6±0.5	472±23	13±1.2	72±15
10	400±13	0.87±0.02	41.4±0.5	1050±53	28±2.4	193±40
5	506±9	0.28±0.01	13.2±0.7	384±64	9.5±1.2	37±20

5	427±2	0.37±0.01	17.6±0.4	491±29	12.5±1.5	65±15
5	366±20	0.65±0.06	30.9±3	778±22	22.5±1.9	160±19
1	363±30	0.11±0.01	5.5±0.1	150±12	4.7±0.3	26±10
1	205±7	0.36±0.03	17.1±1.3	405±68	13±2	67±10
1	150±5	0.67±0.04	32±3	700±50	23±2.3	107±9
Acid-treated fiber						
1	130±8	0.71±0.02	33.8	1622±265	74±6.7	135±21

References

(1)   Bergman, T. L.; Incropera, F. P.; Lavine, A. S., *Fundamentals of Heat and Mass Transfer*. Seventh ed.; John Wiley & Sons: **2011**.